Inorg. Chem. **2005**, *44*, 9360–9368

Cobalt-Containing Silicotungstate Sandwich Dimer $[\{Co_3(B\text{-}\beta\text{-}SiW_9O_{33}(OH))(B\text{-}\beta\text{-}SiW_8O_{29}(OH)_2)\}_2]^{22-}$

Bassem S. Bassil,[†] Ulrich Kortz,*[,†] Anca S. Tigan,[†] Juan M. Clemente-Juan,*[,‡] Bineta Keita,[§] Pedro de Oliveira,[§] and Louis Nadjo*[,§]

School of Engineering and Science, International University Bremen, P. O. Box 750 561, 28725 Bremen, Germany, Instituto de Ciencia Molecular, Universidad de Valencia, C/Dr. Moliner 50, 46100-Burjassot, Valencia, Spain, and Laboratoire de Chimie Physique, UMR 8000, CNRS, Equipe d'Electrochimie et Photoélectrochimie, Université Paris-Sud, Bâtiment 420, 91405 Orsay Cedex, France

Received September 11, 2005

The 6-cobalt-substituted $[\{Co_3(B\text{-}\beta\text{-}SiW_9O_{33}(OH))(B\text{-}\beta\text{-}SiW_8O_{29}(OH)_2)\}_2]^{22-}$ (**1**) has been characterized by IR and UV–vis spectroscopy, elemental analysis, magnetic studies, electrochemistry, and gel filtration chromatography. A single-crystal X-ray analysis was carried out on $K_{10}Na_{12}[\{Co_3(B\text{-}\beta\text{-}SiW_9O_{33}(OH))(B\text{-}\beta\text{-}SiW_8O_{29}(OH)_2)\}_2]\cdot 49H_2O$ (**KNa-1**), which crystallizes in the monoclinic system, space group $P2_1/n$, with $a = 19.9466(8)$ Å, $b = 24.6607(10)$ Å, $c = 34.0978(13)$ Å, $\beta = 102.175(1)°$, and $Z = 2$. Polyanion **1** represents a novel class of asymmetric sandwich-type polyanions. It contains three cobalt ions, which are encapsulated between an unprecedented ($B\text{-}\beta\text{-}SiW_9O_{34}$) fragment and a ($B\text{-}\beta\text{-}SiW_8O_{31}$) unit. Polyanion **1** is composed of two sandwich species via two Co–O–W bridges in the solid state and almost certainly in solution as well based on gel filtration chromatography. UV–visible spectroscopy and cyclic voltammetry also confirmed its stability. Two well-separated groups of waves appeared in the voltammetric pattern: the wave observed in the negative potential range versus a saturated calomel electrode features the redox processes of W^{VI} centers; the two reversible redox couples observed in the positive potential domain are attributed to the redox processes of Co^{2+} centers and indicated that the two types of Co^{2+} centers in the structure are oxidized in separate waves. Such reversibility of Co^{2+} centers within multi-Co-substituted polyoxometalates is uncommon. The magnetic properties of **KNa-1** are also discussed. The ferromagnetic ground state has been studied by magnetic susceptibility and magnetization measurements and fitted according to an anisotropic exchange model.

Introduction

Polyoxometalates (POMs) are discrete, molecular metal–oxygen clusters with an unmatched structural variety combined with a multitude of properties.[1−4] Sometimes they are referred to as soluble metal oxide fragments, which indicates their intermediate nature between classical coordination chemistry and solid-state science. The search for novel POMs is predominantly driven by the exciting catalytic, medicinal, magnetic, electronic, and optical properties of many transition-metal-substituted polyoxotungstates. For example, the catalytic activity of such POMs in the oxidation of organic substrates by a variety of oxidants (e.g., O_2, H_2O_2, and air)

* Author to whom correspondence should be addressed. E-mail: u.kortz@iu-bremen.de. Fax: (+49)421-200 3229.
† International University Bremen.
‡ Universidad de Valencia.
§ Université Paris-Sud.

(1) Pope, M. T. *Heteropoly and Isopoly Oxometalates*; Springer: Berlin, 1983.
(2) (a) Pope, M. T.; Müller, A. *Angew. Chem., Int. Ed. Engl.* **1991**, *30*, 34. (b) Pope, M. T.; Müller, A. *Polyoxometalates: from Platonic Solids to Anti Retroviral Activity*; Kluwer: Dordrecht, The Netherlands, 1994. (c) Hill, C. L.; Prosser-McCartha, C. M. *Coord. Chem. Rev.* **1995**, *143*, 407. (d) *Chem. Rev.* **1998**, *98*, 1−389 (Special Thematic Issue on Polyoxometalates). (e) Pope, M. T.; Müller, A. *Polyoxometalate Chemistry: From Topology via Self-Assembly to Applications*; Kluwer: Dordrecht, The Netherlands, 2001. (f) *Polyoxometalate Chemistry for Nano-Composite Design* (Eds.: Yamase, T., Pope, M. T.), Kluwer: Dordrecht, **2002.** (g) Pope, M. T. *Comput. Coord. Chem. II* **2003**, *4*, 635. (h) Hill, C. L. *Comput. Coord. Chem. II* **2003**, *4*, 679. (i) Borrás-Almenar, J. J.; Coronado, E.; Müller, A.; Pope, M. T. *Polyoxometalate Molecular Science*; Kluwer: Dordrecht, The Netherlands, 2004.
(3) Berzelius, J. *Poggendorf's Ann. Phys.* **1826**, *6*, 369.
(4) (a) Keggin, J. F. *Nature* **1933**, *131*, 908. (b) Keggin, J. F. *Proc. R. Soc. London, Ser.A* **1934**, *144*, 75.

10.1021/ic0515554 CCC: $30.25
Published on Web 10/29/2005

combined with a high thermal stability have led to industrial applications.[2b,d−f] Transition-metal-substituted polyoxotungstates can also be of interest for their magnetic properties.[2b,d−f] Structures that contain more than one paramagnetic transition metal ion in close proximity may exhibit exchange-coupled spins.

Within the class of transition-metal-substituted POMs, the sandwich-type compounds represent the largest subclass.[5] To date the Weakley-, Hervé-, Krebs-, and Knoth-type sandwich structures can be distinguished. Synthesis of such compounds is usually accomplished by the reaction of a transition metal ion (e.g., Cu^{2+}, Mn^{2+}) with the appropriate lacunary POM precursor (e.g., $[As^{III}W_9O_{33}]^{9-}$, $[GeW_9O_{34}]^{10-}$, and $[P_2W_{15}O_{56}]^{12-}$). Usually, the structure of the lacunary POM precursor is preserved in the sandwich-type polyanion products.

Predominantly, our group has shown that this is not the case for the divacant decatungstosilicate, $[\gamma\text{-}SiW_{10}O_{36}]^{8-}$, which was first reported by Hervé et al. about 20 years ago.[6] In our hands, the reaction of $[\gamma\text{-}SiW_{10}O_{36}]^{8-}$ with a variety of first-row transition metals has led to dimeric ($[\{\beta\text{-}SiNi_2W_{10}O_{36}(OH)_2(H_2O)\}_2]^{12-}$, $[M_4(H_2O)_2(B\text{-}\alpha\text{-}SiW_9O_{34})_2]^{12-}$ [M = Mn^{2+}, Cu^{2+}, Zn^{2+}]), trimeric $\{[(\beta_2\text{−}SiW_{11}MnO_{38}OH)_3]^{15-}\}$, and tetrameric ($[\{\beta\text{-}Ti_2SiW_{10}O_{39}\}_4]^{24-}$) products, and in all cases, the γ-tungsten-oxo framework was not preserved.[7−10] We can conclude that the dilacunary precursor $[\gamma\text{-}SiW_{10}O_{36}]^{8-}$ isomerizes easily in an aqueous, acidic medium upon heating and in the presence of first-row transition metal ions, which can result in oligomeric products with unexpected structures. Therefore, we decided to investigate the $Co^{2+}/[\gamma\text{-}SiW_{10}O_{36}]^{8-}$ system in some detail, as only one structurally characterized cobalt(II)-containing silicotungstate had been reported.[5h]

Very recently, we synthesized the 15-cobalt-substituted polyoxotungstate $[Co_6(H_2O)_{30}\{Co_9Cl_2(OH)_3(H_2O)_9(\beta\text{-}SiW_8O_{31})_3\}]^{5-}$ by interaction of Co^{2+} ions with the dilacunary $[\gamma\text{-}SiW_{10}O_{36}]^{8-}$ in a simple one-pot procedure in an aqueous, acidic NaCl medium.[11] This trimeric polyanion has a core of nine Co^{2+} ions encapsulated by three ($\beta\text{-}SiW_8O_{31}$) fragments and two Cl^- ligands. The highly symmetrical structural core unit $[Co_9Cl_2(OH)_3(H_2O)_9(\beta\text{-}SiW_8O_{31})_3]^{17-}$ is surrounded by six antenna-like $Co^{II}(H_2O)_5$ groups, resulting in a satellite-like structure. The polyanion $[Co_6(H_2O)_{30}\{Co_9Cl_2(OH)_3(H_2O)_9(\beta\text{-}SiW_8O_{31})_3\}]^{5-}$ contains more cobalt ions than any other polyoxotungstate known to date. Interestingly, Mialane et al. reported on an azide-containing Cu(II) derivative with a very similar structural core.[12]

Here, we report on the synthesis, structure, electrochemistry, and magnetism of another novel cobalt(II)-containing silicotungstate.

Experimental Section

Synthesis. All reagents were used as purchased without further purification. The dilacunary precursor $K_8[\gamma\text{-}SiW_{10}O_{36}]$ was synthesized according to the published procedure.[6]

$K_{10}Na_{12}[\{Co_3(B\text{-}\beta\text{-}SiW_9O_{33}(OH))(B\text{-}\beta\text{-}SiW_8O_{29}(OH)_2)\}_2]\cdot 49H_2O$ (KNa-1). A 0.19 g sample of $CoCl_2\cdot 6H_2O$ (0.79 mmol) was dissolved in 20 mL of a 0.5 M sodium acetate buffer at pH 4.8 followed by the addition of 1.0 g (0.36 mmol) of $K_8[\gamma\text{-}SiW_{10}O_{36}]$. The solution was stirred for 30 min at 50 °C and then was allowed to cool to room temperature and filtered. Then, 1 mL of a 1 M KCl solution was added to the filtrate, and the solution was allowed to evaporate at room temperature. After about 2 weeks, purple crystals suitable for X-ray diffraction had formed (yield 0.17 g, 38%). It should be noted that, even without the addition of KCl solution, crystals of **KNa-1** are formed. However, this process can be accelerated by the addition of potassium ions. Furthermore, the same polyanion **1** can be obtained if the above reaction is performed in water at pH 4.8, keeping everything else the same. In fact, we discovered that **1** can be synthesized up to pH 7.0 as monitored by IR spectroscopy on precipitated solids. IR for **KNa-1**: 989(sh), 945(m), 885(s), 847(s), 789(m), 723(s), 619(sh), 534(w), 493(w) cm^{-1}. Anal. Calcd for **KNa-1**: K, 3.8; Na, 2.7; W, 60.4; Co, 3.4; Si, 1.1. Found: K, 3.7; Na, 3.0; W, 61.2; Co, 3.3; Si, 1.3. The elemental analysis was performed by Kanti Labs Ltd. in Mississauga, Canada.

X-ray Crystallography. A purple, irregular block of **KNa-1** with dimensions $0.14 \times 0.10 \times 0.06$ mm^3 was mounted on a glass fiber for indexing and intensity data collection at 173 K on a Bruker D8 SMART APEX CCD single-crystal diffractometer using Mo Kα radiation (λ = 0.710 73 Å). Of the 40 824 unique reflections ($2\theta_{max} = 56.66°$), 17 543 reflections ($R_{int} = 0.161$) were considered observed [$I > 2\sigma(I)$]. Direct methods were used to solve the structure and to locate the tungsten and cobalt atoms (SHELXS-97). Then, the remaining atoms were found from successive difference maps (SHELXL-97). The final cycle of refinement, including the atomic coordinates, anisotropic thermal parameters (W, Co, Si, Na, and K atoms), and isotropic thermal parameters (O atoms), converged at $R = 0.060$ and $R_w = 0.145$ [$I > 2\sigma(I)$]. In the final difference map, the deepest hole was -2.242 $eÅ^{-3}$ and the highest peak was 6.643 $eÅ^{-3}$. Routine Lorentz and polarization corrections were applied, and an absorption correction was performed using the SADABS program.[13] Crystallographic data are summarized in Table 1.

UV−Visible Spectroscopy. Pure water was used throughout. It was obtained by passing it through a RiOs 8 unit followed by a Millipore-Q Academic purification set. All reagents were of high-purity grade and were used as purchased without further purification. The UV−visible spectra were recorded on a Perkin−Elmer Lambda

(5) Representative examples include the following and references therein: (a) Bi, L.-H.; Kortz, U. *Inorg. Chem.* **2004**, *43*, 7961. (b) Bi, L.-H.; Reicke, M.; Kortz, U.; Keita, B.; Nadjo, L.; Clark, R. J. *Inorg. Chem.* **2004**, *43*, 3915. (c) Kortz, U.; Nellutla, S.; Stowe, A. C.; Dalal, N. S.; Rauwald, U.; Danquah, W.; Ravot, D. *Inorg. Chem.* **2004**, *43*, 2308. (d) Kortz, U.; Nellutla, S.; Stowe, A. C.; Dalal, N. S.; van Tol, J.; Bassil, B. S. *Inorg. Chem.* **2004**, *43*, 144. (e) Keita, B.; Mbomekalle, I. M.; Nadjo, L.; Anderson, T. M.; Hill, C. L. *Inorg. Chem.* **2004**, *43*, 3257. (f) Ritorto, M. D.; Anderson, T. M.; Neiwert, W. A.; Hill, C. L. *Inorg. Chem.* **2004**, *43*, 44. (g) Limanski, E. M.; Drewes, D.; Krebs, B. *Z. Anorg. Allg. Chem.* **2004**, *630*, 523. (h) Laronze, N.; Marrot, J.; Hervé, G. *Inorg. Chem.* **2003**, *42*, 5857. (i) Hussain, F.; Reicke, M.; Janowski, V.; de Silva, S.; Futuwi, J.; Kortz, U. *C. R. Chim.* **2005**, *8*, 1045.
(6) Tézé, A.; Hervé, A. G. *Inorganic Syntheses* **1990**, Vol. 27, p 88.
(7) Kortz, U.; Jeannin, Y. P.; Tézé, A.; Hervé, G.; Isber, S. *Inorg. Chem.* **1999**, *38*, 3670.
(8) Kortz, U.; Isber, S.; Dickman, M. H.; Ravot, D. *Inorg. Chem.* **2000**, *39*, 2915.
(9) Kortz, U.; Matta, S. *Inorg. Chem.* **2001**, *40*, 815.
(10) Hussain, F.; Bassil, B. S.; Bi, L.-H.; Reicke, M.; Kortz, U. *Angew. Chem., Int. Ed.* **2004**, *43*, 3485.
(11) Bassil, B. S.; Nellutla, S.; Kortz, U.; Stowe, A. C.; van Tol, J.; Dalal, N. S.; Keita, B.; Nadjo, L. *Inorg. Chem.* **2005**, *44*, 2659.
(12) Mialane, P.; Dolbecq, A.; Marrot, J.; Rivière, E.; Sécheresse, F. *Chem. Eur. J.* **2005**, *11*, 1771.
(13) Sheldrick, G. M. *SADABS*; Siemens Analytical X-ray Instrument Division: Madison, WI, 1995.

Table 1. Crystal Data and Structure Refinement for $K_{10}Na_{12}[\{Co_3(B\text{-}\beta\text{-}SiW_9O_{33}(OH))(B\text{-}\beta\text{-}SiW_8O_{29}(OH)_2)\}_2]\cdot 49H_2O$ (**KNa-1**)

emp formula	$Co_6H_{104}K_{10}Na_{12}O_{179}Si_4W_{34}$
fw	10352.8
space group (No.)	$P2_1/n$ (14)
a (Å)	19.9466(8)
b (Å)	24.6607(10)
c (Å)	34.0978(13)
β (deg)	102.1750(10)
vol (Å^3)	16395.4(11)
Z	4
temp (°C)	−100
wavelength (Å)	0.71073
d_{calcd} (Mg m^{-3})	4.058
abs coeff (mm^{-1})	24.745
$R\ [I > 2\sigma(I)]^a$	0.057
R_w (all data)^b	0.097

^{a} $R = \sum||F_o|-|F_c||/\sum|F_o|$. ^{b} $R_w = [\sum w(F_o^2-F_c^2)^2/\sum w(F_o^2)^2]^{1/2}$.

19 spectrophotometer on 1.2×10^{-6} M solutions of **KNa-1**. Matched 1.000 cm optical-path quartz cuvettes were used. The compositions of the various media were as follows: for pH 0, HCl; for pH 5, 0.4 M $CH_3COONa + CH_3COOH$; for pH 7, 0.4 M NaH_2PO_4 + NaOH.

Gel Filtration Chromatography. A 1 mL mixture of 1 mM each of $[P_8W_{48}O_{184}]^{40-}$ (**P_8W_{48}**), $[P_2W_{15}Mo_2VO_{62}]^{8-}$ (**$Mo_2VP_2W_{15}$**), and $[\{Co_3(B\text{-}\beta\text{-}SiW_9O_{33}(OH))(B\text{-}\beta\text{-}SiW_8O_{29}(OH)_2)\}_2]^{22-}$ (**1**) in a 1 M LiCl solution was passed through a 40 cm × 1 cm^2 Sephadex G-50 fine column previously equilibrated in the same solution. Sephadex G-50 separates molecules ranging in molecular mass M_r from 500 to 10 000, the largest being eluted first. The migration and concomitant separation of the colored products (**1**, pink, and **$Mo_2VP_2W_{15}$**, blue) down the column was easily followed by visual inspection. Fractions of approximately 2 mL were collected and analyzed by UV−visible−NIR spectrophotometry with a Perkin−Elmer Lambda 19 spectrophotometer, which allowed the monitoring of the elution of the three products, each having its characteristic spectrum with strong absorption bands in the UV region. The same procedure was repeated both in pure water and in a 0.4 M sodium acetate/acetic acid buffer, pH = 5.00 (the latter being one of the buffers used in the electrochemical experiments), with a 1 mL mixture of 1 mM each of **1** and **$Mo_2VP_2W_{15}$**, the outcome being the same as for the experiment in 1 M LiCl.

Electrochemical Experiments. The concentration of **1** was 2×10^{-4} M. The solutions were de-aerated thoroughly for at least 30 min with pure argon and kept under a positive pressure of this gas during the experiments. The source, mounting, and polishing of the glassy carbon (GC, Tokai, Japan) electrodes has been described.[14] The glassy carbon samples had a diameter of 3 mm. The electrochemical setup was an EG & G 273 A driven by a PC with the M270 software. Potentials are quoted against a saturated calomel electrode (SCE). The counter electrode was a platinum gauze of large surface area. All experiments were performed at room temperature.

Magnetic Properties. Variable temperature susceptibility measurements were carried out on a polycrystalline sample of **KNa-1** in the temperature range 2−300 K at different magnetic fields (0.1, 0.5, 1.0, and 2.5 T) with a magnetometer (Quantum Design MPMS-XL-5) equipped with a SQUID sensor. The susceptibility data were corrected from the diamagnetic contributions as deduced by using Pascal's constant tables. Isothermal magnetization measurements at low temperatures (2 and 5 K) were performed up to 5 T in the same apparatus.

Results and Discussion

Synthesis and Structure. Reaction of Co^{2+} ions with $[\gamma\text{-}SiW_{10}O_{36}]^{8-}$ in a ratio of 2:1 in an acetate buffer medium (pH 4.8) at 50 °C resulted in the novel, dimeric sandwich assembly $[\{Co_3(B\text{-}\beta\text{-}SiW_9O_{33}(OH))(B\text{-}\beta\text{-}SiW_8O_{29}(OH)_2)\}_2]^{22-}$ (**1**), see Figure 1. This polyanion is composed of two equivalent sandwich fragments which are arranged almost orthogonally to each other. Interestingly, each sandwich fragment is built up of two different Keggin units. One of them is the ($B\text{-}\beta\text{-}SiW_8O_{34}$) fragment, which we had observed for the first time very recently in another Co^{2+}-containing silicotungstate.[11] The other Keggin unit is the ($B\text{-}\beta\text{-}SiW_9O_{34}$) fragment, which has never been observed before in polyanion chemistry. These two different Keggin units are held together by three cobalt(II) ions, resulting in an asymmetric (C_1 symmetry) sandwich structure with the hypothetical formula $[Co_3(H_2O)(B\text{-}\beta\text{-}SiW_9O_{33}(OH))(B\text{-}\beta\text{-}SiW_8O_{29}(OH)_2)]^{11-}$ (**1a**), see Figure 2. Our single-crystal X-ray diffraction results show that, in the solid-state, two molecules of **1a** are connected via two equivalent Co−O−W′ bonds leading to the dimeric **1**. The "outer" cobalt ion of one sandwich fragment is connected via an oxo bridge to a belt-tungsten atom from a nonrotated triad of the ($B\text{-}\beta\text{-}SiW_9O_{34}$) unit of the other sandwich fragment. Interestingly, in the case of **1**, always two identical enantiomers of **1a** (*dd* or *ll*) are linked, resulting in a chiral assembly of C_2 symmetry. However, as both enantiomers are present in equal amounts in the solid state, the polyanion crystallizes in a centrosymmetric space group ($P2_1/n$). We have evidence that **1** exists even in aqueous solutions after redissolution of the solid material **KNa-1**, as based on gel chromatography and electrochemistry (see below).

The dimeric **1** is unprecedented in transition-metal-substituted POM chemistry. The only other structurally characterized cobalt(II)-containing silicotungstates known to date are Hervé's $[K_2\{Co(H_2O)_2\}_3(A\text{-}\alpha\text{-}SiW_9O_{34})_2]^{12-}$ and our Co-15-containing $[Co_6(H_2O)_{30}\{Co_9Cl_2(OH)_3(H_2O)_9(\beta\text{-}SiW_8O_{31})_3\}]^{5-}$.[5h,11] Nevertheless, there is one other class of polyanions that is structurally, but not compositionally, similar to **1**. These are the mixed-valence heteropoly brown species $[H_4BW^{IV}{}_3W^{VI}{}_{17}O_{66}]^{11-}$ and the isopoly brown species $[H_6W^{IV}{}_3W^{VI}{}_{17}O_{66}]^{11-}$, both reported by Dickman et al. in 2000.[15] These polyanions are also of the asymmetric sandwich type, but they are composed of a ($B\text{-}\alpha\text{-}XW_9O_{34}$) Keggin fragment and a ($\beta\text{-}W_8O_{30}$) isopoly fragment. Furthermore, the composition of the central section of Dickman's heteropoly browns is very different from **1**. Instead of three cobalt ions, there are three reduced W^{IV} centers.

Bond valence sum calculations indicate that the dimeric sandwich assembly **1** is hexaprotonated.[16] The oxygens O8C2, O147, O156, O25C, O273, and O324 are all monoprotonated (see Figure 1). In fact, they are all μ_2-hydroxo

(14) Keita, B.; Girard, F.; Nadjo, L.; Contant, R.; Canny, J.; Richet, M. J. *Electroanal. Chem.* **1999**, *478*, 76.

(15) Dickman, M. H.; Ozeki, T.; Evans, H. T., Jr.; Rong, C.; Jameson, G. B.; Pope, M. T. *J. Chem. Soc., Dalton Trans.* **2000**, 149.

(16) Brown, I. D.; Altermatt, D. *Acta Crystallogr., Sect. B* **1985**, *41*, 244.

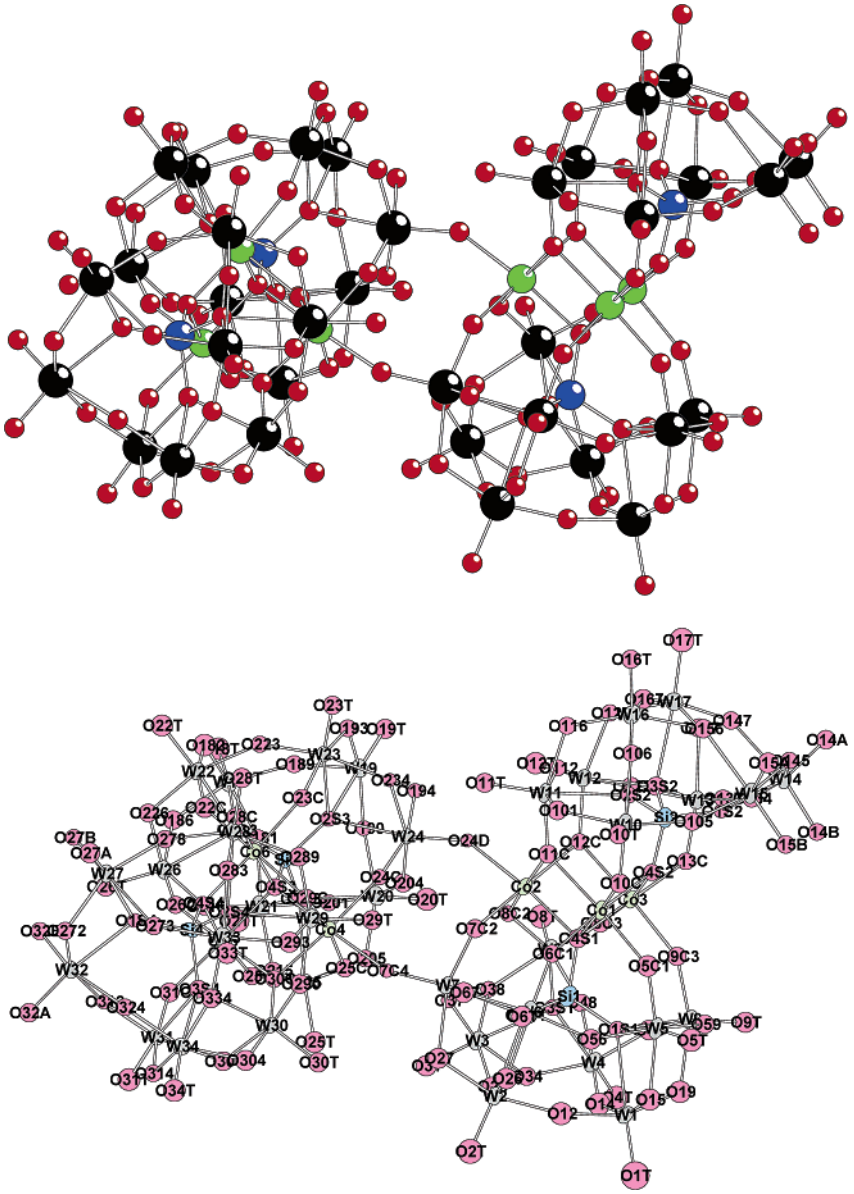

Figure 1. Ball and stick presentation of the sandwich dimer $[\{Co_3(B\text{-}\beta\text{-}SiW_9O_{33}(OH))(B\text{-}\beta\text{-}SiW_8O_{29}(OH)_2)\}_2]^{22-}$ (**1**). The color code is as follows: tungsten (black), cobalt (green), silicon (blue), and oxygen (red). The lower figure shows **1** with thermal ellipsoids (50%) and the labeling scheme.

bridges and can be divided into three groups: The symmetry equivalent O8C2 and O25C are bridging between a cobalt and a tungsten center (Co2−O8C2−W8, Co4−O25C−W25) of the rotated triad within each of the two (B-β-SiW_9O_{34}) fragments in **1**. The oxygen atoms O156 and O273 are symmetry equivalent and so are O147 and O324. They are all bridging between two tungsten centers (W15−O156−W16, W27−O273−O33 and W14−O147−W17, W32−O324−W34) within each of the two (B-β-SiW_8O_{31}) fragments. The atoms W14, W15, W27, and W32 represent the four tungsten centers in **1** with two terminal oxo ligands. Interestingly this reduces the total negative charge of **1** to −22, which means that the monomeric sandwich fragment **1a** would have exactly the same charge of −11 as Dickman's mixed-valence clusters $[H_4BW^{IV}{}_3W^{VI}{}_{17}O_{66}]^{11-}$ and $[H_6W^{IV}{}_3W^{VI}{}_{17}O_{66}]^{11-}$. We also learn that, in **1**, the (B-β-SiW_8O_{31}) fragment is more basic than the (B-β-SiW_9O_{34}) unit as, in the former, two W−O−W bridges are protonated, whereas, in the latter, only one Co−O−W bridge is protonated. This means that it might be possible to extend the structure of **1** via the condensation of additional metal-oxo units onto these basic sites.

The structure of polyanion **1** can be considered as an intermediate during formation of the well-known Weakley-type sandwich structure $[M_4(H_2O)_2(B\text{-}\alpha\text{-}SiW_9O_{34})_2]^{n-}$. In 2000, our group reported on the manganese(II), copper(II), and zinc(II) derivatives $[M_4(H_2O)_2(B\text{-}\alpha\text{-}SiW_9O_{34})_2]^{12-}$ (M = Mn^{2+}, Cu^{2+}, Zn^{2+}), and all three species were synthesized from $[\gamma\text{-}SiW_{10}O_{36}]^{8-}$ using conditions very similar to those of **1**.[8] It must be remembered that formation of the Weakley dimer (which contains B-α-SiW_9O_{34} units) from the $[\gamma$-$SiW_{10}O_{36}]^{8-}$ precursor requires isomerization ($\gamma \rightarrow \beta \rightarrow \alpha$) and a loss of tungsten. Most likely, the (B-β-SiW_9O_{34}) and (B-β-SiW_8O_{31}) fragments observed in **1** are intermediate transformation products of (γ-$SiW_{10}O_{36}$) → (B-α-SiW_9O_{34}). Both fragments, which are probably very unstable as free,

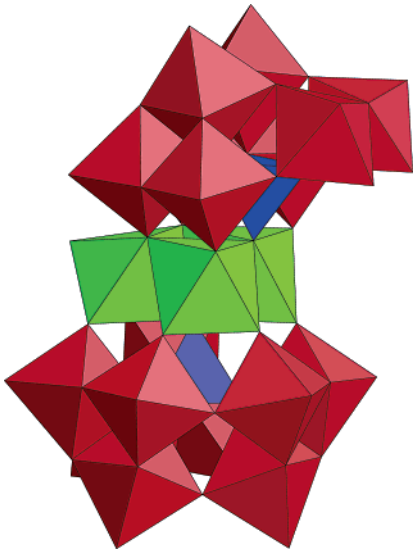

Figure 2. Polyhedral presentation of the half-unit of **1** with the molecular formula $[Co_3(H_2O)(B\text{-}\beta\text{-}SiW_9O_{33}(OH))(B\text{-}\beta\text{-}SiW_8O_{29}(OH)_2)]^{11-}$ (**1a**). The polyhedra represent WO_6 (red), CoO_6 (green), and SiO_4 (blue).

lacunary ions, are most likely trapped in the monomeric **1a** first, which then dimerizes to the more stable **1**. Interestingly, we never isolated analogues of **1** or **1a** for any other first-row transition metal besides cobalt. This indicates that the interaction of Co^{2+} ions with $[\gamma\text{-}SiW_{10}O_{36}]^{8-}$ is very different from the other divalent transition metal ions Mn^{2+}, Cu^{2+}, and Zn^{2+}. In fact, the behavior of Co^{2+} with $[\gamma\text{-}SiW_{10}O_{36}]^{8-}$ in an acidic, aqueous medium resembles somewhat that of Ni^{2+}. For the $Ni^{2+}/[\gamma\text{-}SiW_{10}O_{36}]^{8-}$ system, we also did not observe the formation of the Weakley dimer, but we rather isolated a Keggin dimer structure containing the novel (β-$SiW_{10}O_{37}$) fragment, $[\{\beta\text{-}SiNi_2W_{10}O_{36}(OH)_2(H_2O)\}_2]^{12-}$.[7]

It is also of interest to compare the structures and synthesis conditions of **1** and Co-15-containing $[Co_6(H_2O)_{30}\{Co_9Cl_2(OH)_3(H_2O)_9(\beta\text{-}SiW_8O_{31})_3\}]^{5-}$.[11] Both species are cobalt(II)-containing silicotungstates and both contain the novel (B-β-SiW_8O_{31}) fragment. Close inspection of the structural core of **1** reveals that it is composed of three fused (Co_3SiW_8) fragments, which are also a building block of **1**. Not surprisingly, polyanions **1** and $[Co_6(H_2O)_{30}\{Co_9Cl_2(OH)_3(H_2O)_9(\beta\text{-}SiW_8O_{31})_3\}]^{5-}$ have very similar synthesis conditions regarding the ratio and concentration of the reagents, solvent, temperature, time of heating, and pH. However, what differs in both are two crucial elements: the counterions and the presence/absence of chloride ions. The Co-15-containing $[Co_6(H_2O)_{30}\{Co_9Cl_2(OH)_3(H_2O)_9(\beta\text{-}SiW_8O_{31})_3\}]^{5-}$ forms only as a sodium salt and requires the presence of chloride ions. On the other hand, the formation of **1** requires the presence of a relatively high concentration of potassium ions. As expected, we were also able to synthesize **1** in a 1 M KCl solution as based on IR results. This observation re-emphasizes the importance of countercations and anions during the formation process of polyanions and not only for crystallization purposes. A full understanding and, above all, control of all parameters that have an impact on polyanion formation is still far away.

In summary, we suggest that the overall transformation (γ-$SiW_{10}O_{36}$) → (B-α-SiW_9O_{34}) proceeds stepwise and involves the following intermediate fragments: (γ-$SiW_{10}O_{36}$) → (β-$SiW_{10}O_{38}$)/(β-$SiW_{10}O_{37}$) → (B-β-SiW_9O_{34})/(B-β-SiW_8O_{31}) → (B-α-SiW_9O_{34}). We notice that, in this transformation, the number of lacunary sites increases, but in our opinion, the main driving force is the conversion from γ- → β- → α-type rotational isomers. The most interesting and probably the most important aspect of our work with the dilacunary precursor $[\gamma\text{-}SiW_{10}O_{36}]^{8-}$ is the fact that only specific 3d transition metal ions can stabilize the above Keggin fragments. Specifically, Ti^{4+} stabilizes (β-$SiW_{10}O_{38}$) in $[\{\beta\text{-}Ti_2SiW_{10}O_{39}\}_4]^{24-}$, Ni^{2+} stabilizes (β-$SiW_{10}O_{37}$) in $[\{\beta\text{-}SiNi_2W_{10}O_{36}(OH)_2(H_2O)\}_2]^{12-}$, Co^{2+} stabilizes (B-β-SiW_9O_{34})/(B-β-SiW_8O_{31}) in **1** and (B-β-SiW_8O_{31}) in $[Co_6(H_2O)_{30}\{Co_9Cl_2(OH)_3(H_2O)_9(\beta\text{-}SiW_8O_{31})_3\}]^{5-}$, and finally, Mn^{2+}, Cu^{2+}, and Zn^{2+} all stabilize (B-α-SiW_9O_{34}) in $[M_4(H_2O)_2(B\text{-}\alpha\text{-}SiW_9O_{34})_2]^{12-}$.[7-11]

Considering that **1** contains two well-separated cobalt-oxo triangles, this species is of interest for electrochemistry/catalysis and magnetism studies.

Electrochemistry and Gel Filtration Chromatography. *The Stability of **1** in Solution.* The stability of **1** was assessed by monitoring its UV−vis spectrum as a function of pH over a period of at least 24 h. Between pH = 0 and 7, all the spectra were reproducible with respect to absorbances and wavelengths. In this domain, the spectrum of **1** was characterized by two relatively broad peaks: the first one remained located between 340 and 350 nm and the second one between 360 and 370 nm. These peaks were better defined when the pH decreased. A complementary cross-check of this suggested stability was obtained by cyclic voltammetry: the same solution could be kept and used for 3 days without any modification in the voltammetric characteristics of the complex. All these observations suggest that **1** was stable in solution, a feature supported by the estimation of its molecular mass in solution.

Estimation of the Molecular Mass by Gel Filtration Chromatography. Gel filtration chromatography is a reliable technique to estimate the molecular mass.[17] In this work, it was used to check whether the title polyanion exists indeed as a dimer ($[\{Co_3(B\text{-}\beta\text{-}SiW_9O_{33}(OH))(B\text{-}\beta\text{-}SiW_8O_{29}(OH)_2)\}_2]^{22-}$; **1**) or perhaps as a monomer $[Co_3(H_2O)(B\text{-}\beta\text{-}SiW_9O_{33}(OH))(B\text{-}\beta\text{-}SiW_8O_{29}(OH)_2)]^{11-}$; **1a**) in solution. Assuming that all the countercations and water molecules separate from the core anion when the solid crystals are put in aqueous solution, the largest species in solution will either be the sandwich monomer **1a** or the sandwich dimer **1**, having ionic masses of 4420 and 8803 g/mol, respectively. These can be undoubtedly distinguished by gel filtration provided that appropriate molecular mass standards are used in the experiments. For Sephadex G-50, which separates species ranging from 500 to 10 000 g/mol, two well-known POMs were chosen as standards: $\mathbf{P_8W_{48}}$ and $\mathbf{Mo_2VP_2W_{15}}$, whose anions have molecular masses of 12 000 and 4200

(17) Nelson, D. L.; Cox, M. M.; Lehninger, A. L. *Principles of Biochemistry*, 3rd ed.; Worth Publishers: New York, 2000.

Figure 3. Photograph of the Sephadex G-50 column taken just a few minutes after the sample mixture was charged. Two distinct colored bands have already separated and correspond to $\mathbf{Mo_2VP_2W_{15}}$ (blue) and **1** (pink), with the latter eluting first.

g/mol, respectively. The major advantage of this choice is the fact that, if **1** were indeed a dimer in solution, its molar mass would fall right between those of the standards and their separation would be expected to be straightforward. In addition, both **1** and $\mathbf{Mo_2VP_2W_{15}}$ are colored, the former being pink and the latter dark blue, which allows the elution of these two species to be easily monitored by simple visual inspection. If the title polyanion **1** happened to be a monomer in solution (that is, **1a**), the pink and dark blue bands in the Sephadex G-50 column, corresponding to **1a** and $\mathbf{Mo_2VP_2W_{15}}$, respectively, would probably not be resolved, taking into account their very close molecular masses (4420 vs 4200 g/mol). A single colored band would be observed in this case. In any case, $\mathbf{P_8W_{48}}$ is eluted before the other species because of its larger molar mass, but it presents two major drawbacks: it requires a high salt concentration in order to dissolve in water (1 M LiCl in the present case), and it is colorless (although it absorbs in the UV range, which renders its detection a rather simple task).

Figure 3 shows a photograph of the Sephadex G-50 column taken while the sample mixture was being separated. Two bands are clearly seen, the dark blue one being closer to the top than the pink one. Since these two species were effectively separated by gel filtration chromatography under the present experimental conditions, it may be concluded that their molecular masses are rather different and that **1** is indeed a dimer in solution. The spectra in Figure S1 (see Supporting Information), corresponding to different fractions eluted from the column, confirm that the different species came out in the expected sequence, starting with the largest and ending with the smallest; that is, $\mathbf{P_8W_{48}}$ was eluted first (not shown), then **1** (pink), and finally $\mathbf{Mo_2VP_2W_{15}}$ (blue). Therefore, we consider the species studied in solution in the following as the sandwich dimer **1** with the molecular formula $[\{Co_3(B\text{-}\beta\text{-}SiW_9O_{33}(OH))(B\text{-}\beta\text{-}SiW_8O_{29}(OH)_2)\}_2]^{22-}$.

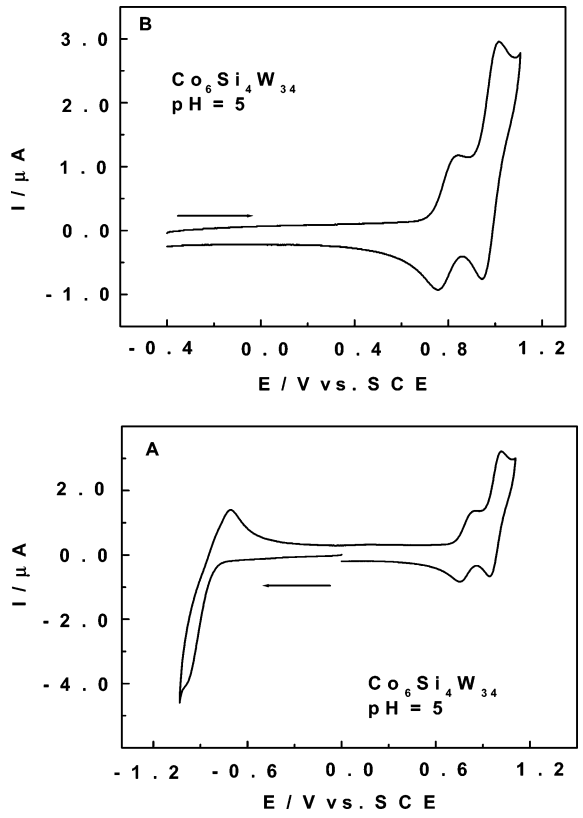

Figure 4. Cyclic voltammogram of 2×10^{-4} M **1** in a pH 5 medium (0.4 M $CH_3COONa + CH_3COOH$). The scan rate was 10 mV s^{-1}, the working electrode was glassy carbon, and the reference electrode was SCE. (A) The whole voltammetric pattern. (B) The voltammetric pattern restricted to the Co^{2+} redox processes.

Cyclic Voltammetry (CV) Characterization. Figure 4 shows the CV of **1** in a pH = 5 medium (0.4 M $CH_3COONa + CH_3COOH$). The pattern is restricted to reversible waves observed in the electroactive range of the supporting electrolyte. Two groups of waves appear in Figure 4A, one of them located in the positive and the other in the negative potential domain versus SCE. The wave observed in the negative potential range ($E_{pc} = -0.980$ V and $E_{pa} = -0.710$ V vs SCE) features the redox processes of W^{VI} centers and is located in the domain where analogous W-based processes were also obtained in banana-shaped or sandwich-type POMs.[5,18] Two reversible redox couples are observed in the positive potential domain with $E_{pa1} = +0.830$ V and $E_{pc1} = +0.760$ V for the first one and $E_{pa2} = +1.016$ V and $E_{pc2} = +0.946$ V for the second one. Both systems are attributed to the redox processes of Co^{2+} centers. We have checked that the electrochemical characteristics of these redox couples are independent of the direction of the initial potential scan. For example, Figure 4B displays the pattern obtained when the potential scan program was never extended to reach the reduction domain of W^{VI} centers. The importance of this observation stems from the following possible analogy with other POMs. It is known that the reduction of several α-Keggin anions $[X^{n+}O_4W_{12}O_{36}]^{[8-n]-}$ ($X = H_2^{2+}$, B^{3+}, Si^{4+}) by at least six electrons, at fairly negative potentials, gives

(18) Jabbour, D.; Keita, B.; Mbomekalle, I. M.; Nadjo, L.; Kortz, U. *Eur. J. Inorg. Chem.* **2004**, 2036.

tungsten "brown" species $[X^{n+}O_4(H_2O)_3W^{IV}{}_3W^{VI}{}_9O_{33}]^{[8-n]-}$, which, on potential reversal, show an irreversible oxidation wave at a potential that is substantially more positive than their formation potential.[1,19] No such observation is made here. Figure 4B indicates clearly that the obtained pattern is independent of the reduction products of W centers. Provisionally, we note that the whole voltammetric patterns in Figure 4 (parts A and B) remain perfectly reproducible upon repeated potential cycling. Controlled potential coulometry was used to confirm that the waves observed in the positive potential domain pertain to the oxidation−reduction of Co^{2+} centers. For this purpose, an initial electrolysis was carried out at +0.85 V, a potential just positive of the first wave peak potential. The oxidation consumes 2.02 electrons per molecule, and the solution turns from pink to a pale peach color. This solution is stable in an argon atmosphere. Its cyclic voltammmogram was run from +0.85 to +1.20 V and indicated that the second Co^{2+} wave had kept its voltammetric characteristics unaltered. Then, a second electrolysis was carried out at +1.0 V on the same solution (second oxidation wave in Figure 4). The solution color remained the same but became deeper and deeper as the electrolysis proceeded. This electrolysis consumed 4.1 electrons per molecule. This result complies with the current intensity ratio that could be deduced from Figure 4. These observations together indicate that all the Co^{2+} centers were oxidized to the Co^{3+} state. The separation of this process into two distinct waves is likely to be linked with the difference in nature between the two types of Co^{2+} present in the framework; thus, the first of these waves in the positive potential direction would feature the redox behavior of the two structurally identical Co^{2+} centers and give a two-electron wave; the second wave, with four electrons, would correspond to the other four Co^{2+} centers. To our knowledge, such an observation of electrochemically well-behaved and reversible Co^{2+} centers in multi-cobalt-substituted POMs is unprecedented.

A final point deserves emphasis: the anodic-to-cathodic peak potential difference for each of these multielectron waves was 0.070 V. In other words, the associated systems behave roughly as one-electron systems, except for current intensities. These observations suggest that the Co^{2+} ions in each of the two types of environments are largely independent and are reduced simultaneously, a feature reminiscent of that encountered with polymers and dendrimers.[1,19,20]

Magnetic Studies. Magnetic susceptibility data for the sandwich dimer polyanion **1** are shown in Figure 5a as a plot of the product $\chi_m T$ versus T at 0.1, 0.5, 1.0, and 2.5 T. At room temperature, $\chi_m T$ has a value of 27.2 emu K/mol, and it decreases upon cooling and reaches a minumum at 38.0 K with a value of 23.4 emu K/mol. Below this temperature, a sharp peak is observed with a maximum at 10.3 K for 0.1 T and a value of 24.8 emu K/mol. This maximum depends on the magnetic field and decreases in value, becomes broader, and shifts to high temperatures when the magnetic field increases. The decrease at high temperatures is due to the spin−orbit coupling of Co^{2+}, while the maximum at low temperatures is indicative of the ferromagnetic $Co^{2+}-Co^{2+}$ interactions within the trinuclear spin cluster. The low-temperature isothermal magnetization versus H curves are plotted in Figure 5b. Because of the high anisotropy of the ferromagnetic ground state, these curves do not follow a Brillouin's function behavior.

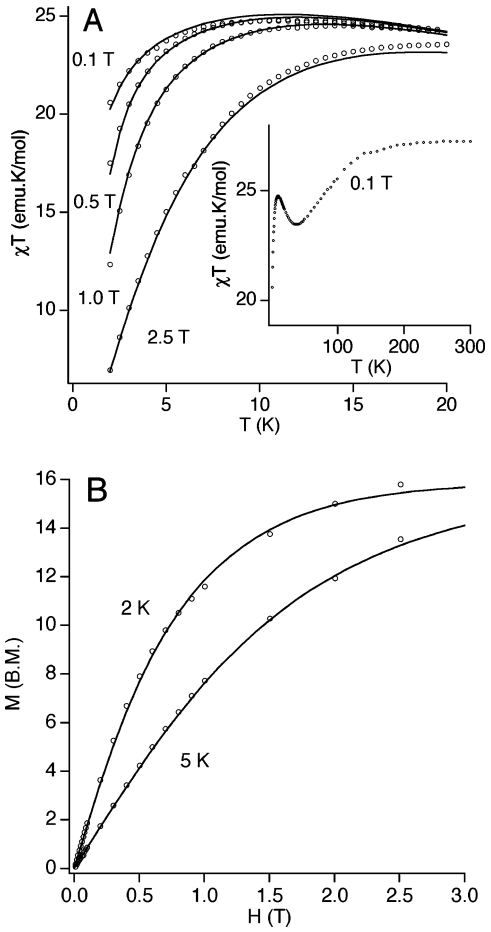

Figure 5. (A) Thermal behavior of $\chi_m T$ for **KNa-1** at different fields: 0.1, 0.5, 1, and 2.5 T. (inset) Experimental $\chi_m T$ of the same sample at 0.1 T in the temperature range 2−300 K. (B) Magnetization vs field for **KNa-1** at 2 and 5 K, respectively. The solid lines in A and B represent the best fitting with the anisotropic model used.

The exchange network of this Co^{2+} cluster involves only one kind of exchange pathway, J, if we suppose that the three Co^{2+} ions form an equilateral triangle and the three edge-sharing oxo bridges are equivalent. This kind of interaction involving edge-sharing CoO_6 octahedra leads to Co−O−Co angles close to 90°, which favors the orthogonality of the magnetic orbitals and ferromagnetic exchange.

The $^4T_1$ high-spin ground state of octahedral Co^{2+} shows a first-order spin−orbit coupling and splits into six anisotropic Kramers doublets. At low temperatures (below 25 K), only the lowest Kramers doublet is populated, so that the

(19) (a) Launay, J. P. *J. Inorg. Nucl. Chem.* **1976**, *38*, 807. (b) Hervé, G. *Ann. Chim.* **1971**, *6*, 287. (c) Flanagan, J. B.; Margel, S.; Bard, A. J.; Anson, F. C. *J. Am. Chem. Soc.* **1978**, *100*, 4248. (d) Smith, T. W.; Kuder, J. E.; Wychick, D. *J. Polym. Sci.* **1976**, *14*, 2433. (e) Saji, T.; Pasch, N. F.; Webber, S. E.; Bard, A. J. *J. Phys. Chem.* **1978**, *82*, 1101. (f) Mbomekalle, I. M.; Keita, B.; Nierlich, M.; Kortz, U.; Berthet, P.; Nadjo, L. *Inorg. Chem.* **2003**, *42*, 5143.

(20) (a) Bryce, M. R.; Devonport, W.; Goldenberg, L. M. *J. Chem. Soc., Chem. Commun.* **1998**, 945. (b) Alonzo, B.; Astruc, D.; Blais, J.-C.; Nlate, S.; Rigaud, S.; Ruiz, J.; Valerio, C. *C. R. Acad. Sci., Ser. IIc: Chim.* **2001**, *4*, 173.

exchange interaction between two Co^{2+} ions can be described by assuming a coupling between these fully anisotropic Kramers doublets with effective spins of $^1/_2$. Expressing this spin anisotropy in terms of exchange anisotropy gives the effective exchange Hamiltonian for our Co^{2+} complex

$$\hat{H} = -2 \sum_{\alpha=x,y,z} J_\alpha (\hat{S}_1^\alpha \hat{S}_2^\alpha + \hat{S}_1^\alpha \hat{S}_3^\alpha + \hat{S}_2^\alpha \hat{S}_3^\alpha)$$

A simultaneous fit of the four magnetic susceptibilities at different fields was performed by numerical diagonalization of the eigenmatrix[21] and gives us the following set of parameters: $J_z = 12.1\ cm^{-1}$, $J_{xy} = 10.6\ cm^{-1}$, $g_z = 5.27$, and $g_{xy} = 5.01$ ($R = 1.4 \times 10^{-2}$). The validity of the anisotropic exchange model developed here is further confirmed by the low-temperature behavior of the magnetization as a function of the external field (Figure 5b).

The sign and magnitude of the exchange parameters for **KNa-1** are in good agreement with those of the three related Co(II)-containing polyoxotungstates $[Co_4(H_2O)_2(PW_9O_{34})_2]^{10-}$,[22a] $[Co_3W(H_2O)_2(CoW_9O_{34})_2]^{12-}$,[22b] and $[(NaOH_2)Co_3(H_2O)(P_2W_{15}O_{56})_2]^{17-}$.[22c] These polyanions exhibit exchange coupling via the edge-shared CoO_6 octahedra in the range $J_z = 8.4-12.9\ cm^{-1}$. The similar magnitudes of the coupling constants for the above Co-containing polyoxotungstates can be rationalized by the very similar bond lengths and angles within the magnetic core of the POMs. At the same time, this means that the magnetic properties of POMs with a Co-containing core do not depend much on the shape (e.g., Keggin vs Wells−Dawson) and composition (tungstophosphate vs tungstosilicate) of the capping tungsten-oxo units. Furthermore, it does not seem to play a major role at all if the sandwich-type POM is symmetric (i.e., contains two identical Keggin caps such as in $[Co_4(H_2O)_2(PW_9O_{34})_2]^{10-}$) or asymmetric (i.e., contains two different Keggin caps such as in **1**). In summary, lacunary Keggin or Wells−Dawson capping fragments represent rigid, diamagnetic units which are ideal for the encapsulation of paramagnetic, exchange-coupled metal-oxo clusters.

Conclusions

We have prepared the cobalt-containing silicotungstate sandwich dimer $[\{Co_3(B\text{-}\beta\text{-}SiW_9O_{33}(OH))(B\text{-}\beta\text{-}SiW_8O_{29}(OH)_2)\}_2]^{22-}$ (**1**) in a simple, one-pot reaction in an aqueous, acidic medium. Polyanion **1** is composed of two asymmetric sandwich subunits which are each composed of three cobalt ions being encapsulated between an unprecedented (B-β-SiW_9O_{34}) fragment and a (B-β-SiW_8O_{31}) fragment. Two of these sandwich subunits are linked via two Co−O−W bridges in an approximately orthogonal fashion, resulting in the novel polyanion assembly **1**. We believe that the dimeric nature of **1** is maintained in solution as based on gel filtration chromatography.

The work presented here reinforces earlier results by our group highlighting the flexible nature of the dilacunary precursor $[\gamma\text{-}SiW_{10}O_{36}]^{8-}$ when it encounters different 3d transition metal ions in aqueous solutions. We have shown that such reactions can lead to unprecedented and unexpected polyanion architectures. Also, Co^{2+} ions react with $[\gamma\text{-}SiW_{10}O_{36}]^{8-}$, leading to novel polyanion structures, which cannot be obtained with any other transition metal ions. This behavior resembles the interaction of Ni^{2+} ions with $[\gamma\text{-}SiW_{10}O_{36}]^{8-}$ because, for this system, we also obtained a unique silicotungstate structure ($[\{\beta\text{-}SiNi_2W_{10}O_{36}(OH)_2(H_2O)\}_2]^{12-}$) containing the unprecedented (β-$SiW_{10}O_{37}$) fragment.

Future synthetic work in this area will be focused on the discovery of other transition-metal-substituted silicotungstate structures with a potential for homogeneous and heterogeneous oxidation catalysis. We will focus on redox-active 3d metals (e.g., Fe^{3+}, Cr^{3+}) and also on 4d and 5d metals (e.g., Ru^{3+}, Pd^{2+}). Of particular interest are open polyanion structures with accessible transition metal centers. We believe that by using the $[\gamma\text{-}SiW_{10}O_{36}]^{8-}$ precursor we have a good chance of discovering fundamentally novel polyanion architectures. Finally, we are also interested in preparing diamagnetic analogues of our novel compounds, to study their solution properties by NMR in addition to electrochemistry.

In addition to the experimental proof of the dimeric structure of **1** in solution, several remarkable observations were made during the electrochemical characterization of this complex. The two types of Co^{2+} centers which can be distinguished in the structure of **1** are oxidized in separate waves, creating a mixed-valence species. These waves are well-behaved, with an anodic-to-cathodic peak potential difference that suggests simultaneous one-electron oxidation of the centers belonging to the same group. Such reversibility of Co^{2+} centers in multi-cobalt-substituted POMs is uncommon and deserves emphasis. Furthermore, the stability of **1** and its electrochemical behavior open up the way for catalytic and electrocatalytic applications, the pathways of which might be amenable to simple interpretations.

The low-temperature magnetic properties of **1** have also been studied and explained according to an anisotropic exchange model. The magnitude of the ferromagnetic exchange parameter is similar to those of other Co(II)-containing POMs. In the future, we plan a detailed inelastic neutron scattering investigation of **KNa-1**, which can help us to understand the anisotropic exchange interactions of the title polyanion **1** in more detail.

Acknowledgment. U.K. thanks the International University Bremen for research support and the Florida State University Chemistry Department (U. S. A.) for allowing him unlimited access to the single-crystal X-ray diffractometer. This work was also supported by the CNRS (UMR 8000) and the University Paris-Sud XI. Figures 1−2 were

(21) (a) Borrás-Almenar, J. J.; Clemente-Juan, J. M.; Coronado, E.; Tsukerblat, B. S. *Inorg. Chem.* **1999**, *38*, 6081. (b) Borrás-Almenar, J. J.; Clemente-Juan, J. M.; Coronado, E.; Tsukerblat, B. S. *J. Comput. Chem.* **2001**, *22*, 985.

(22) (a) Andres, H.; Clemente-Juan, J. M.; Aebersold, M.; Güdel, H. U.; Coronado, E.; Büttner, H.; Kearly, G.; Melero, J.; Burriel, R. *J. Am. Chem. Soc.* **1999**, *121*, 10028. (b) Clemente-Juan, J. M.; Coronado, E.; Gaita-Arinñoo, A.; Giménez-Saiz, C.; Chaboussant, G.; Güdel, H.-U.; Burriel, R.; Mutka, H. *Chem. Eur. J.* **2002**, *8*, 5701. (c) Clemente-Juan, J. M.; Coronado, E.; Gaita-Arinñoo, A.; Giménez-Saiz, C.; Güdel, H.-U.; Sieber, A.; Bircher, R.; Mutka, H. *Inorg. Chem.* **2005**, *44*, 3389.

generated by Diamond Version 2.1e (copyright Crystal Impact GbR). J.M.C.-J. thanks the MCyT for a Ramón y Cajal contract.

Supporting Information Available: One X-ray crystallographic file in CIF format. Visible spectra of four different fractions eluted from the Sephadex G-50 column equilibrated with a 0.4 M sodium acetate/acetic acid buffer, pH = 5.00 (one figure). This material is available free of charge via the Internet at http://pubs.acs.org.

IC0515554